

# Modification of Polypropylene and Polypropylene/Fibrous Cellulose Composites by the Addition of Poly(ethylene oxide)

Hisayuki Nakatani, Kensuke Miyazaki

Department of Biotechnology and Environmental Chemistry, Kitami Institute of Technology, 165 Koen-Cho, Kitami, Hokkaido, Japan 090-8507

Received 7 April 2008; accepted 2 November 2008

DOI 10.1002/app.29623

Published online 6 March 2009 in Wiley InterScience (www.interscience.wiley.com).

**ABSTRACT:** Effects of the addition of poly(ethylene oxide) (PEO) on the tensile properties of a polypropylene (PP)/fibrous cellulose (FC) composite were studied. PEO was incompatible with the PP matrix, and a PP/PEO blend showed a sea-island morphology. However, the existence of the PEO phase hardly impaired the ductility of PP, leading to a strain constraint relaxation resulting from void formation in the phase. The tensile behavior of PP/PEO was little affected by the content (until 10 wt %) or molecular weight of PEO. The results suggested that the PEO phase was able to be deformed in a slit-like shape and had no interaction with the PP matrix. Effects of PEO on the morphology and tensile and fracture behavior of the PP/FC composite with maleated polypro-

pylene (MAPP) as a compatibilizer critically depended on the preparation method. In the case of the addition of PEO to PP/FC/MAPP, increases in the strain and fracture energy were observed in comparison with PP/FC. In the case of the addition of FC/PEO to PP/MAPP, although the obtained composite showed a lower Young's modulus and tensile strength in comparison with PP/FC, the strain and fracture energy were considerably increased by the existence of the PEO layer coating the FC. © 2009 Wiley Periodicals, Inc. *J Appl Polym Sci* 112: 3362–3370, 2009

**Key words:** composites; modification; polyolefins; toughness

## INTRODUCTION

Cellulose is the most abundant polymer material in the world and has been used as a raw material for building materials and paper for a long time. Its advantages are its low cost, high modulus, renewability, and biodegradability. Cellulose also has attracted much attention from many researchers for use in composite materials.<sup>1–7</sup> In particular, their attention has recently been concentrated on its high modulus and renewability from the viewpoints of both mechanical and environmental advantages. A composite based on cellulose has been considered a useful way of taking advantage of the existing features. In general, milled wood materials have been used as composite cellulose materials. Such wood materials are commonly called wood flour or fibrous cellulose (FC).

The most popular example of such composites is a combination with polypropylene (PP).<sup>1,4–7</sup> This is due to the commercial importance of PP as an applicable material for household appliances, medical wares, and automotive and other industrial pro-

ducts. Moreover, in the PP composite, FC has been explored as an alternative to glass and carbon fibers and as a biodegradable material. The PP/FC composite is, however, quite brittle. Improvement of the mechanical properties is required.

It is well known that the addition of an elastomer is effective in improving the toughness of a brittle polymer.<sup>8–12</sup> The improvement method can be similarly applied for PP.<sup>13,14</sup> In the case of PP, an incompatible polymer, such as a styrene–ethylene–butadiene–styrene triblock copolymer, has been used as the additive elastomer.<sup>14</sup> If there exists an appropriate elastomer, the improvement method would be applicable for the PP/FC composite. Poly(ethylene oxide) (PEO) is regarded as one applicable elastomer because it is typically incompatible with PP<sup>15,16</sup> and has high flexibility. In addition, both PEO and cellulose are hydrophilic, and the formation of hydrogen bonds is feasible between them.<sup>17</sup> A nanocomposite<sup>18</sup> and a thermoplastic composite<sup>19</sup> of cellulose and PEO can be prepared with the hydrogen bonds. The existence of the hydrogen bonds will bring about distinctly different properties for the PP/FC composite.

The purpose of this study was to clarify the effects of the addition of PEO on the morphology and tensile properties of PP and the PP/FC composite. For the PP/PEO polymer blend, the dependence of the PEO content and its molecular weight were studied.

Correspondence to: H. Nakatani (nakatani@chem.kitami-it.ac.jp).

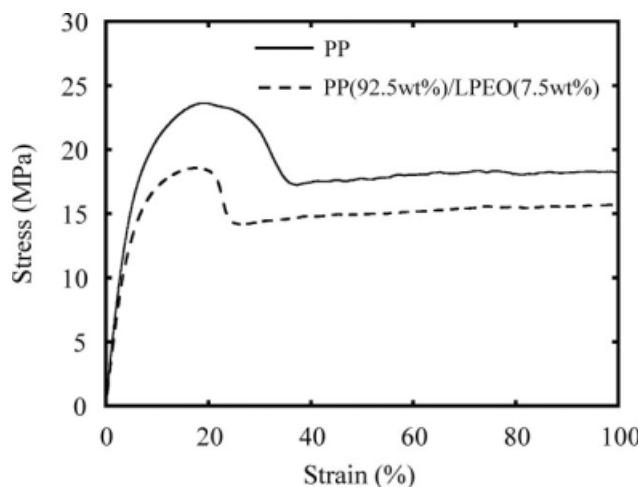


Figure 1 Stress-strain curves of PP and PP/LPEO.

For the PP/FC composite, the effects of the difference in the PEO addition method on the morphology and tensile behavior were studied.

## EXPERIMENTAL

### Materials

PP (mesopentad fraction = 98%) was supplied by Japan Polypropylene Co. (Yokkaichi, Japan). The number-average molecular weight and polydispersity (weight-average molecular weight/number-average molecular weight) of PP were  $4.6 \times 10^4$  and 5.7, respectively.

Two kinds of PEOs were purchased from Wako Pure Chemical Industries, Ltd. (Osaka, Japan). The PEOs with lower (20,000) and higher (500,000) average molecular weights were denoted LPEO and HPEO, respectively.

FC (W-100GK) was donated by Nippon Paper Chemicals Co., Ltd. (Tokyo, Japan). The moisture of the FC was below 0.7 wt %. The dimensions were over 90% through a 100-mesh screen, and the average length was about 37  $\mu\text{m}$ . The FC was dried in a desiccator for 7 days before preparation.

Maleated polypropylene (MAPP; maleic anhydride content  $\approx 8$  wt %), used as a compatibilizer, was purchased from Sigma-Aldrich (St. Louis, MO). The number-average molecular weight and polydispersity (weight-average molecular weight/number-average molecular weight) of MAPP were  $3.9 \times 10^3$  and 2.3, respectively. MAPP is a very popular compatibilizer for PP composites. In the PP/FC composite, the availability of MAPP is well known.<sup>1,4,6</sup> Therefore, MAPP was used as the compatibilizer in this study.

### Preparation of the PP/PEO polymer blend

The polymer blend was prepared with an Imoto Seisakusyo (Kyoto, Japan) IMC-1884 melting mixer. After a small amount of a phenolic antioxidant (AO-60, Adekastab;  $\sim 0.5$  wt %) was added, the mixing was performed. The mixing conditions were 180°C at 60 rpm for 5 min in the LPEO addition, whereas they were 210°C at 60 rpm for 5 min in the HPEO addition. These samples were molded into a film (100  $\mu\text{m}$ ) by compression molding at 190°C under 5 MPa for 5 min and were quenched at 20°C. The obtained samples were dried in a desiccator over 1 day before the measurement and testing.

### Preparation of the PP/FC composites

The PP/FC composites were classified into two types according to the difference in the sequence of mixing. In the case of the composite denoted PP/MAPP/FC+LPEO, PP, MAPP, and FC were first mixed, and then LPEO was added. For LPEO/FC+PP/MAPP, LPEO and FC were first mixed, and then PP and MAPP were added. These PP/FC composites were prepared with an Imoto Seisakusyo IMC-1884 melting mixer. After a small amount of a phenolic antioxidant (AO-60, Adekastab;  $\sim 0.5$  wt %) was added, the mixing was performed. The mixing conditions were 180°C at 60 rpm for 5 min. The samples were molded into films (100  $\mu\text{m}$ ) by compression molding at 190°C under 5 MPa for 5 min and were quenched at 20°C. The obtained samples

TABLE I  
Mechanical Properties of Various PP Blend Samples

| Sample                         | Young's modulus (MPa) | Tensile strength (MPa) | Elongation at break (%) |
|--------------------------------|-----------------------|------------------------|-------------------------|
| PP                             | 370 $\pm$ 10          | 23.6 $\pm$ 0.4         | >200 <sup>a</sup>       |
| PP (97.5 wt %)/LPEO (2.5 wt %) | 319 $\pm$ 24          | 19.3 $\pm$ 0.4         | >200 <sup>a</sup>       |
| PP (92.5 wt %)/LPEO (7.5 wt %) | 318 $\pm$ 23          | 18.8 $\pm$ 0.3         | >200 <sup>a</sup>       |
| PP (90 wt %)/LPEO (10 wt %)    | 291 $\pm$ 9           | 18.6 $\pm$ 0.5         | >200 <sup>a</sup>       |
| PP (92.5 wt %)/HPEO (7.5 wt %) | 328 $\pm$ 11          | 18.8 $\pm$ 0.6         | >200 <sup>a</sup>       |

<sup>a</sup> The samples did not break under the tensile testing conditions (until an elongation of 200%).

were dried in a desiccator over 1 day before the measurement and testing.

### Tensile testing

Stress–strain behavior was observed with a Shimadzu (Tokyo, Japan) EZ-S at a crosshead speed of 5 mm/min. The sample specimens were cut with dimensions of  $30 \times 2 \times 0.1$  mm,<sup>3</sup> and the gauge length was 10 mm. We chose the specialized specimen (like the ISO reed shape) to adapt to the size of our tensile testing machine. All tensile testing was performed at 20°C. All results were the average values of five measurements.

### Single-edge-notch (SEN) tensile test

The fracture behavior was studied with an SEN test. The method of van der Wal and Gaymans<sup>20</sup> was used as the reference. The SEN test was carried out on a Shimadzu EZ-S at a crosshead speed of 5 mm/min with a strip specimen ( $30 \times 2 \times 0.1$  mm<sup>3</sup>) having a single-edge, 45°, V-shaped notch (tip radius = 0.3 mm). Although the SEN test of van der Wal and Gaymans was carried out with a standard dumbbell-shaped sample (ISO R27-1:  $10 \times 3 \times 115$  mm<sup>3</sup>) with a V-shaped notch (tip radius = 0.25 mm), we chose the specialized specimen because of the smaller size of our tensile testing machine. All results were the average values of five measurements.

### Wide-angle X-ray diffraction (WAXD) measurement and procedure for the crystallinity calculation

WAXD diffractograms were recorded in reflection geometry at 2° (2 $\chi$ /min) under Ni-filtered Cu K $\alpha$  radiation with a Rigaku Corp. (Tokyo, Japan). XG-

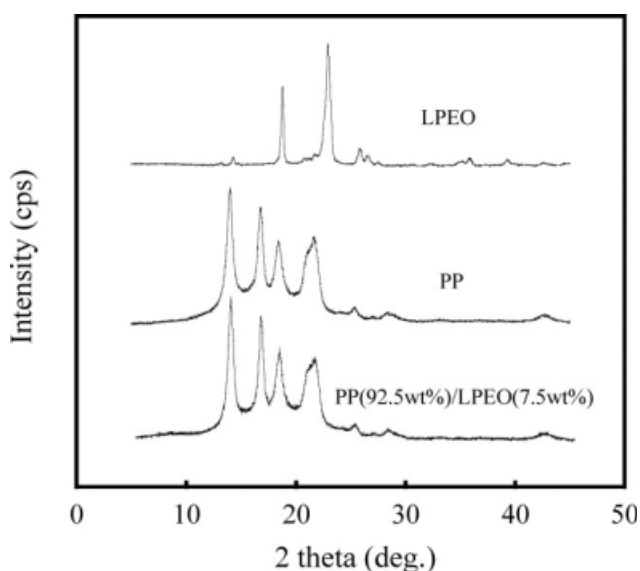


Figure 2 WAXD profiles of PP/LPEO, PP, and LPEO.

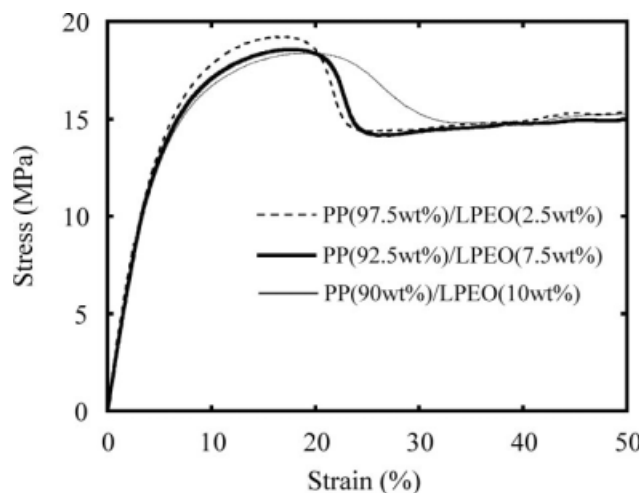


Figure 3 Stress–strain curves of PP/LPEO.

Rint 1200 diffractometer. The crystallinity was estimated from the WAXD peak area, whose calculation was performed with software (Integral Analysis for Windows, version 5.0, Rigaku).

### Scanning electron microscopy (SEM) measurement

The morphology of the composite was examined with a JEOL (Tokyo, Japan) JSM-5800 at 30 kV. The plate of the composite was fractured in liquid nitrogen, and then the fractured surface was sputter-coated with gold.

## RESULTS AND DISCUSSION

Figure 1 shows the stress–strain curve of the PP (92.5 wt %)/LPEO (7.5 wt %) blend. The tensile strength of the PP/LPEO blend is approximately 20% lower than that of the PP; however, the blend exhibits necking behavior and is not broken under

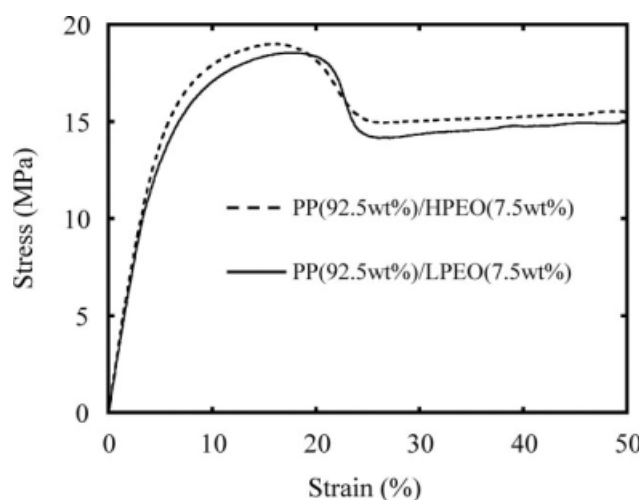
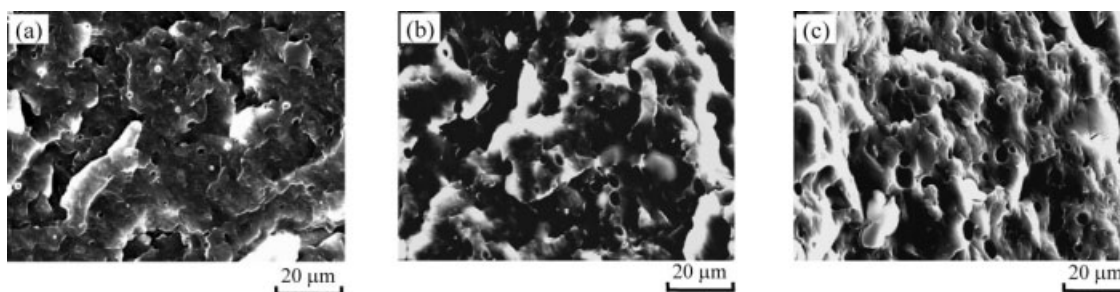


Figure 4 Stress–strain curves of PP/LPEO and PP/HPEO.



**Figure 5** SEM micrographs of fracture surfaces of PP/LPEO: (a) PP (97.5 wt %)/LPEO (2.5 wt %), (b) PP (92.5 wt %)/LPEO (7.5 wt %), and (c) PP (90 wt %)/LPEO (10 wt %).

the experimental conditions, just like the PP (see Table I). The tensile behavior reveals that the addition of PEO hardly impairs the ductility of PP.

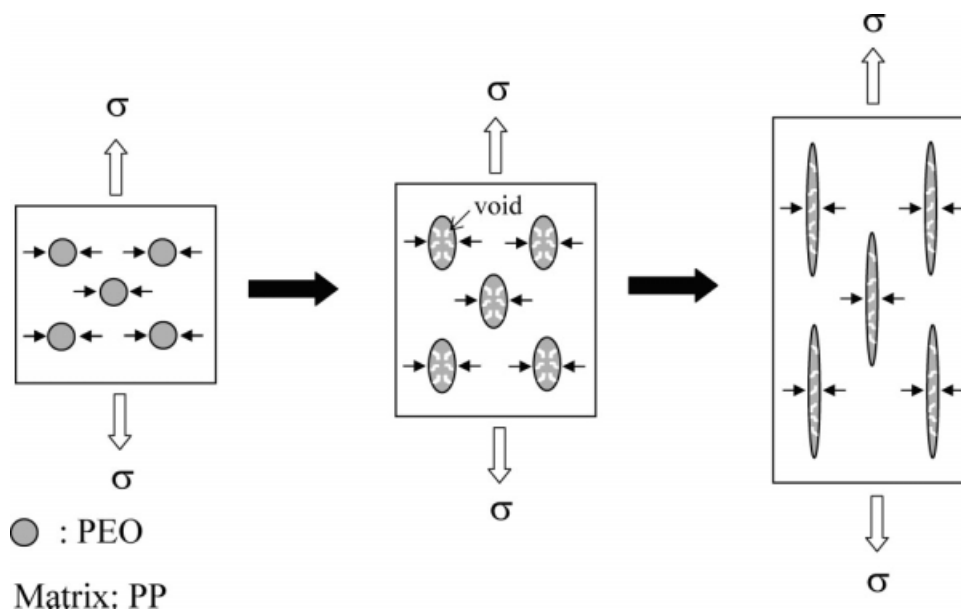
Figure 2 shows the WAXD profiles of PP/LPEO, PP, and LPEO. The crystal form of the PP in the PP (92.5 wt %)/LPEO (7.5 wt %) blend is the  $\alpha$ -form (monoclinic), just like the PP. The WAXD peak corresponding to LPEO is unseen, and the degrees of crystallinity of the PP and PP (92.5 wt %)/LPEO (7.5 wt %) blend are 54 and 50 wt %, respectively. When we consider the existence of LPEO, the crystallinity (50 wt %) is in good agreement with the weight ratio of the PP, that is,  $50/54 \approx 0.925$  (92.5 wt %), in the blend. These results suggest that the addition of LPEO brings about no changes in the crystalline morphology or in the crystallization rate of PP under the blend preparation conditions.

Figure 3 shows the stress–strain curves of blends with various LPEO contents. Although an increase

in the LPEO content seems to cause a slight decrease in the tensile strength and a slight broadness of the yield region, major changes in the mechanical parameters do not appear up to a 10% concentration of LPEO, as summarized in Table I.

The effect of the molecular weight of PEO on the tensile behavior of the PP/PEO blend is shown in Figure 4. The stress–strain curves of PP/LPEO and PP/HPEO are in good agreement with each other, and this indicates that the molecular weight is an independent factor in the tensile behavior of the PP/PEO blend. This implies that there are no other interactions (e.g., chain entanglement) except for the van der Waals force between PP and PEO chains.

SEM micrographs of fractured surfaces of the PP/LPEO blends are shown in Figure 5. The fracture surfaces are quite smooth, having many hemispherical holes, which correspond to the LPEO phase. The size of the holes obviously depends on the LPEO



**Figure 6** Schematic diagram illustrating the tensile deformation mechanism of the PP/PEO blend.



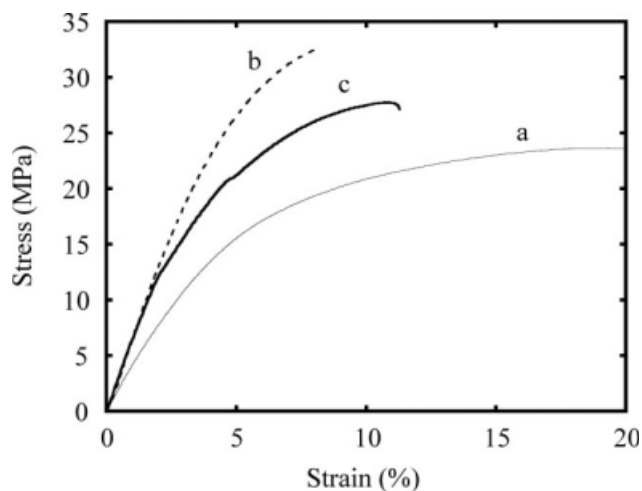


**Figure 7** Stress–strain curves of PP, PP/MAPP/FC, and PP/MAPP/FC+LPEO: (a) PP, (b) PP (69.5 wt %)/MAPP (0.5 wt %)/FC (30 wt %), and (c) PP (62 wt %)/MAPP (0.5 wt %)/FC (30 wt %)+LPEO (7.5 wt %).

content. These phase-separated (sea-island) morphologies indicate that PP and PEO are typically an incompatible blend.<sup>15,16</sup>

Many investigators have reported that employing an incompatible elastomer/polymer blend is effective in improving the toughness of polymer materials.<sup>8–14</sup> The enhanced toughness is believed to be due to a strain constraint relaxation resulting from void formation in the dispersed elastomer phase.<sup>9</sup> In this relaxation mechanism, the elastomer, having lower mechanical strength, is desirable from the structural viewpoint of preferential void formation.<sup>10</sup> It is noted here that the PP/PEO blend sufficiently fulfills such toughening criteria because PEO is a flexible polymer and its mechanical strength is considerably less than that of PP. In addition, although PEO is a crystalline polymer, the elasticity is considerably lower than that of PP. PEO acts as an elastomer in the PP matrix because of its lower elasticity. When tensile stress is applied, the weaker PEO phase is deformed. Many voids are preferentially generated in the PEO phase, leading to the relaxa-

tion of the strain constraint. The PEO phase is more highly deformed by the additionally applied stress and finally ends up as a slit-like shape, as shown in Figure 6. The decrease in the PP/LPEO tensile strength is ascribed to the reduced cross-section area of the PP matrix. The decrease is, however, not proportional to the LPEO content. The cross-section area of the PP matrix slowly decreases against the LPEO content because of the slit-like LPEO deformation. Therefore, the dependence of the tensile strength on the LPEO content would be ambiguous.

The toughening effect with the addition of PEO is not so useful in a ductile polymer such as PP. However, it seems that the effect is very useful for a brittle PP composite such as a PP/cellulose composite.

Figure 7 shows the stress–strain curve of a PP (69.5 wt %)/FC (30 wt %) composite with MAPP (0.5 wt %) as a compatibilizer. Although the tensile strength is considerably higher than that of PP, the tensile behavior is typically brittle. It should be noted here that an increase in strain can be observed with the addition of LPEO to the PP/FC composite. As summarized in Table II, the PP (62 wt %)/MAPP (0.5 wt %)/FC (30 wt %)+LPEO (7.5 wt %) composite has a considerably higher Young's modulus and a higher tensile strength versus PP. Additionally, the composite has about 30% higher elongation at break than that of the composite without LPEO added. This tensile behavior suggests that the toughening is capable of performing with the high stiffness maintained.

The toughening effect can be interpreted if we consider the SEM micrographs in Figure 8, which shows the fractured surfaces of the PP (62 wt %)/MAPP (0.5 wt %)/FC (30 wt %)+LPEO (7.5 wt %) composite. Figure 8 reveals that the FC is tightly coated with the PP/MAPP layer. There are many fine holes in the matrix. These holes are assigned to the LPEO phase and play the role of void points, at which the relaxation of the strain constraint preferentially occurs, as mentioned previously. It has been found that the addition of PEO is an effective method for the improvement of the toughness of PP/cellulose composites.

**TABLE II**  
Mechanical Properties of Various PP Composite Samples

| Sample  | Young's modulus (MPa) | Tensile strength (MPa) | Elongation at break (%) |
|---|-----------------------|------------------------|-------------------------|
| PP  | 370 ± 10              | 23.6 ± 0.4             | >200 <sup>a</sup>       |
| PP (69.5 wt %)/MAPP (0.5 wt %)/FC (30 wt %)               | 628 ± 51              | 30.8 ± 2.7             | 8.4 ± 0.3               |
| PP (62 wt %)/MAPP (0.5 wt %)/FC (30 wt %)+LPEO (7.5 wt %) | 533 ± 22              | 26.8 ± 0.9             | 11.1 ± 0.8              |
| FC (30 wt %)/LPEO (7.5 wt %)+PP (62 wt %)/MAPP (0.5 wt %) | 355 ± 22              | 12.3 ± 1.1             | 30.1 ± 8.1              |

<sup>a</sup> The samples did not break under the tensile testing conditions (until an elongation of 200%).

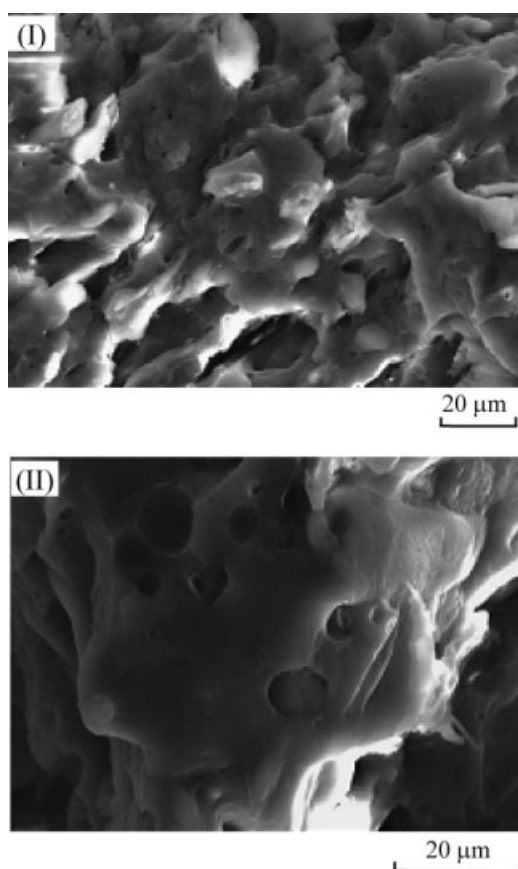


**Figure 8** SEM micrographs of the fracture surface of PP (62 wt %)/MAPP (0.5 wt %)/FC (30 wt %)+LPEO (7.5 wt %): (I)  $\times 1000$  and (II)  $\times 1700$ .

FC and PEO are hydrophilic, and a hydrogen bond is formed between them.<sup>17</sup> The composite can be prepared with this hydrogen bond.<sup>18,19</sup> In this work, the FC/LPEO composite was first prepared

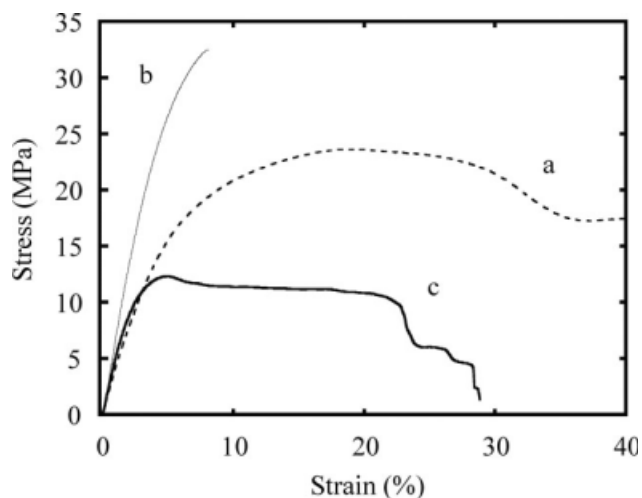


**Figure 9** Stress-strain curves of PP, PP/MAPP/FC, and FC/LPEO+PP/MAPP: (a) PP (69.5 wt %)/MAPP (0.5 wt %)/FC (30 wt %), and (c) FC (30 wt %)/LPEO (7.5 wt %)+PP (62 wt %)/MAPP (0.5 wt %).

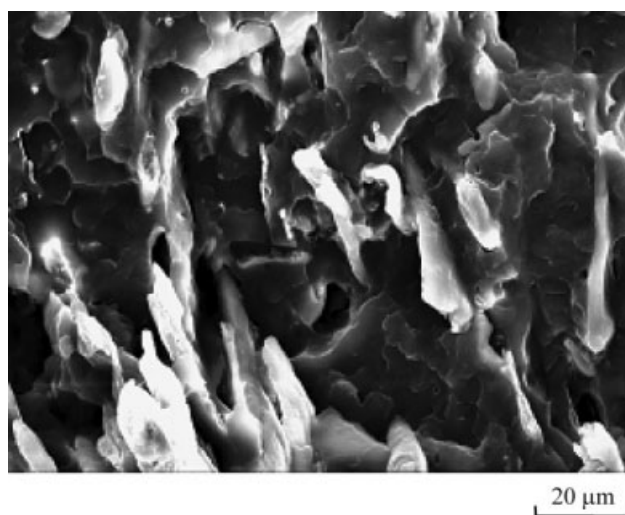


**Figure 10** SEM micrograph of the fracture surface of FC (30 wt %)/LPEO (7.5 wt %)+PP (62 wt %)/MAPP (0.5 wt %).

and was then mixed with PP and MAPP as a compatibilizer. The obtained composite was denoted LPEO/FC+PP/MAPP. The stress-strain curve of FC (30 wt %)/LPEO (7.5 wt %)+PP (62 wt %)/MAPP (0.5 wt %) is shown in Figure 9. Although the values of the Young's modulus and the tensile strength are approximately half of those of PP (69.5 wt %)/MAPP (0.5 wt %)/FC (30 wt %), the value of the elongation at break is approximately 4 times greater (see Table II). In addition, the stress-strain curve is in good agreement with that of PP up to the strain value of 2–3%.

Esterification<sup>1</sup> occurs between the OH group in FC and the maleic anhydride group in MAPP, which is compatible with PP. The existence of the grafted

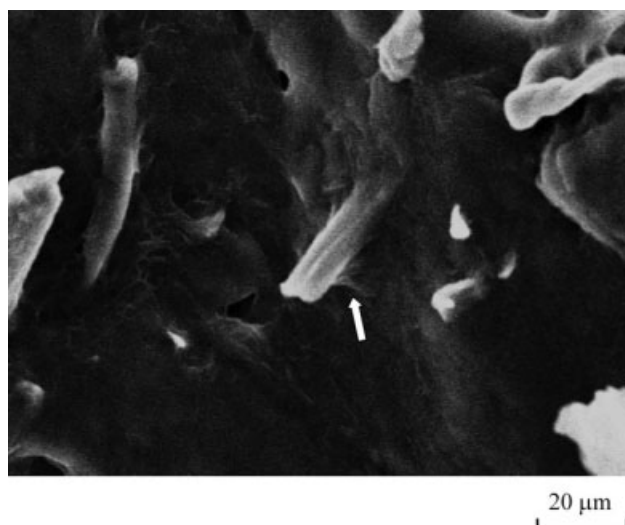


**Figure 11** SEM micrograph of the fracture surface of FC (10 wt %)/LPEO (90 wt %). The arrow indicates the interfacial bond between FC and LPEO.

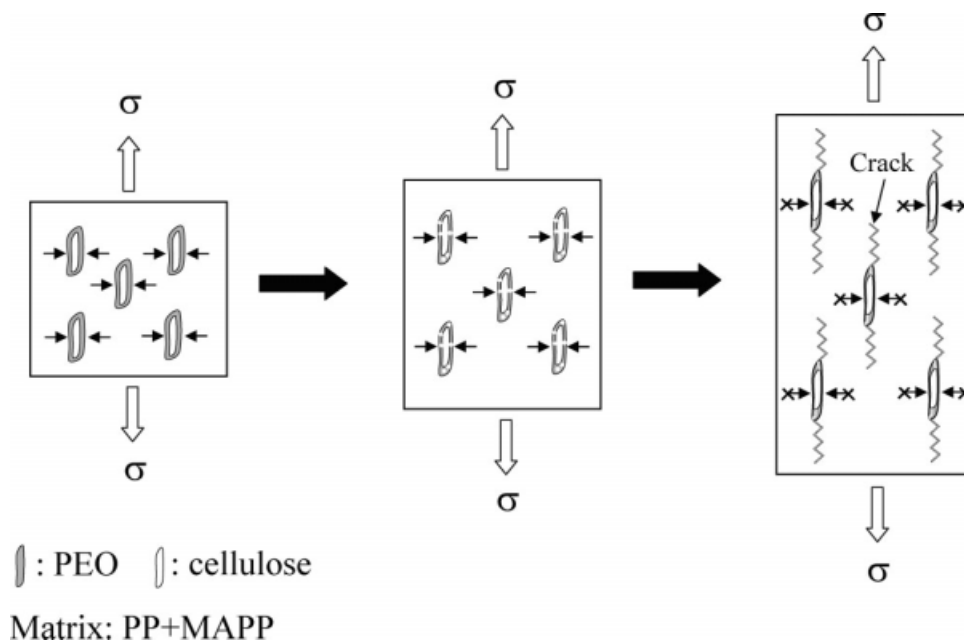


**Figure 12** Schematic diagram illustrating the tensile deformation mechanism of the FC/LPEO+PP/MAPP composite.

MAPP/FC brings about a higher Young's modulus. The PP/MAPP/FC+LPEO composite exhibits a higher Young's modulus because of the formation of the grafted MAPP/FC component. In the case of the FC/LPEO+PP/MAPP composite, the formation of the grafted MAPP/FC would be blocked by LPEO. Therefore, the Young's modulus is low. The higher value of the elongation at break supports the existence of the FC blocked by the LPEO.

Figure 10 shows an SEM micrograph of the fracture surface of FC (30 wt %)/LPEO (7.5 wt %)+PP (62 wt %)/MAPP (0.5 wt %). The coated fibers and the fibrous gaps can be observed. These are the FC/LPEO composite and its imprinted PP matrix. In addition, as shown in Figure 11, the interfacial bond between FC and LPEO can be observed. This suggests that a hydrogen bond is formed between FC and LPEO.<sup>17-19</sup> When tensile stress is applied, the FC/LPEO composite phase is deformed, as shown in Figure 12. Many voids are initially generated in the FC/LPEO phase as well as the PEO phase, leading to the relaxation of the strain constraint. The deformation is, however, restricted by the existence of FC. After the deformation becomes impossible, the applied stress is stored in the form of constrained plasticity in FC and finally overcomes the fibril strength of the PP/MAPP matrix (crack occurrence). There is no interaction between the FC and PP/MAPP matrix because of the covering with the LPEO layer. Therefore, the initial tensile behavior is similar to that of PP (see Table II). In this preparation method, the obtained composite has less tensile strength and higher strain because of the isolated

FC. This suggests that a stiff material at a high concentration (ca. 30 wt %) can be dispersed in the PP matrix without its ductility.

The fracture behavior of the PP/MAPP/FC, PP/MAPP/FC+LPEO, and FC/LPEO+PP/MAPP composites was estimated by SEN testing.<sup>20</sup> As shown in Figure 13, the fracture process can be divided into crack initiation and crack propagation stages.<sup>20</sup> In the crack initiation stage, the stress builds up at the notch tip, but it is too low to enable crack propagation. Here it should be noticed that the crack

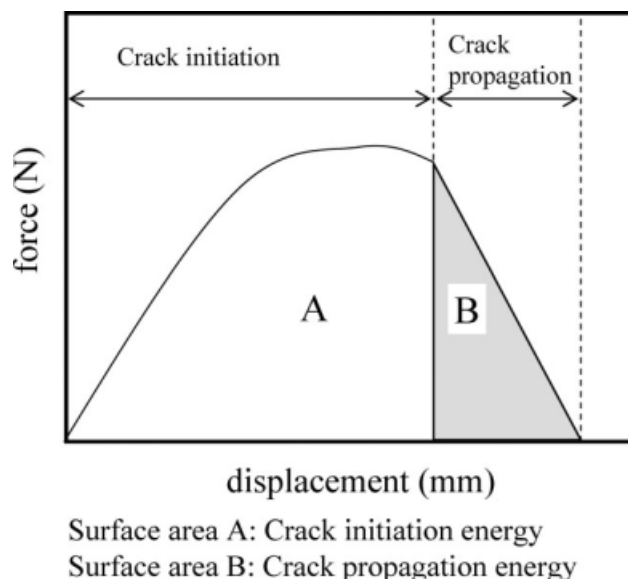


**Figure 13** Schematic force-displacement graph obtained with the SEN tensile test.

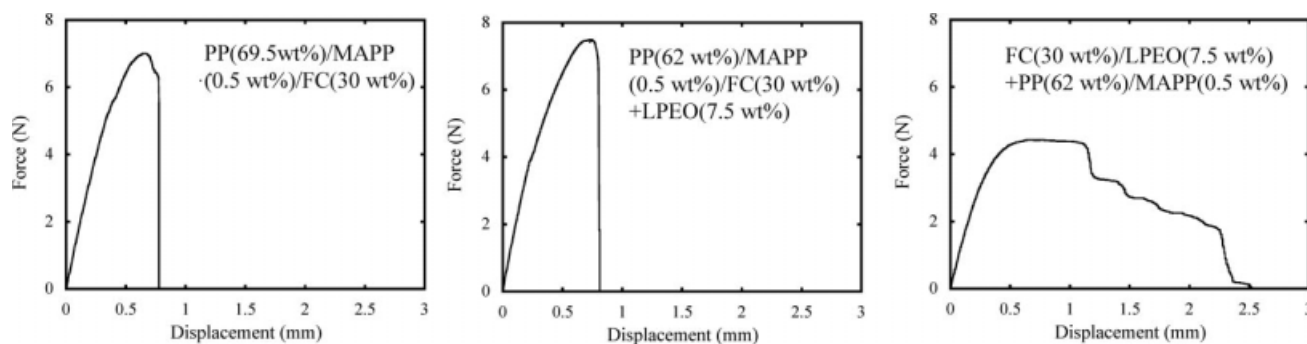


**Figure 14** Force–displacement curves obtained with the SEN tensile test for various composites.

propagation stage is linked to ductility behavior. The crack propagation stage begins at or past the maximum in the stress–displacement curve, and the energy supplied during the crack propagation is a measure of the ductility.<sup>20</sup>

Figure 14 shows the force–displacement curves obtained by SEN testing for these composites. The curve of the FC/LPEO+PP/MAPP composite exhibits the crack propagation region, suggesting that the composition is quite ductile. The fracture energy (surface area of the force–displacement curve) is considerably higher than those of the other compositions (see Table III). This composition has plastic deformation even in the notch. This plastic deformation occurs so that the PP matrix has no interaction with FC. The fracture behavior supports the assumption that there is no interaction between the FC and PP/MAPP matrix because of the covering with the LPEO layer, as mentioned previously. However, the curves of the PP/MAPP/FC and PP/MAPP/FC+LPEO compositions contain no crack propagation regions. Both compositions typically exhibit brittle behavior. However, as shown in Table III, the fracture energy of PP/MAPP/FC+LPEO is slightly higher than that of PP/MAPP/FC, and this indicates that the existence of LPEO brings about an improvement in the fracture toughness of the PP/MAPP/FC composite. Uotila et al.<sup>21</sup> reported that ethylene-pro-

pylene elastomer particles hindered crack propagation in a PP/silica composite.<sup>21</sup> The LPEO particles may play the role as well as the elastomer particles, although the ability to hinder crack propagation is quite low.

## CONCLUSIONS

With the aim of tensile modification of the PP/FC composite, the effects of the addition of PEO on the morphology and tensile properties of PP and PP/FC composites were studied. PEO was incompatible with PP, and its polymer blend exhibited a sea-island morphology. However, the existence of PEO hardly impaired the ductility of PP. The ductility was due to a strain constraint relaxation resulting from void formation in the dispersed PEO phase. The tensile behavior of the PP/PEO blend was little affected by the content (until 10 wt %) or molecular weight of PEO, and this suggested that the PEO phase was deformed into a slit-like shape and had no interaction with the PP matrix.

The effects of PEO on the morphology and tensile and fracture behavior of the PP/FC composite critically depended on the preparation method. In the case of the addition of PEO to the PP/FC composite, increases in the strain and fracture energy were observed in comparison with the PP/FC composite. The increment mechanism was due to the strain constraint relaxation and the hindrance of crack propagation by the separated PEO phase. In the case of the addition of the FC/PEO composite to the PP matrix, although the obtained composite showed a lower Young's modulus and tensile strength versus the PP/FC composites, the strain and fracture energy were considerably increased by the existence of the PEO layer coating the FC.

## References

1. Felix, J. M.; Gatenholm, P. *J Appl Polym Sci* 1991, 42, 609.
2. Hedenberg, P.; Gatenholm, P. *J Appl Polym Sci* 1996, 60, 2377.

**TABLE III**  
Fracture Energies of Various PP Composite Samples

| Sample  | Fracture energy (kJ/m <sup>2</sup> ) <sup>a</sup> |
|---|---|
| PP (69.5 wt %)/MAPP (0.5 wt %)/FC (30 wt %)               | 10.6 ± 0.9  |
| PP (62 wt %)/MAPP (0.5 wt %)/FC (30 wt %)+LPEO (7.5 wt %) | 12.1 ± 0.7  |
| FC (30 wt %)/LPEO (7.5 wt %)+PP (62 wt %)/MAPP (0.5 wt %) | 18.8 ± 2.8  |

<sup>a</sup> Surface area of the force–displacement curves obtained by the SEN tensile test.



3. Zhang, F.; Qiu, W.; Yang, L.; Endo, T. *J Mater Chem* 2002, 12, 24.
4. Qiu, W.; Zhang, F.; Endo, T.; Hirotsu, T. *J Appl Polym Sci* 2003, 87, 337.
5. Qiu, W.; Zhang, F.; Endo, T.; Hirotsu, T. *J Appl Polym Sci* 2004, 91, 1703.
6. Qiu, W.; Zhang, F.; Endo, T.; Hirotsu, T. *J Appl Polym Sci* 2004, 94, 1326.
7. Hristov, V. N.; Vasileva, S. T.; Krumova, M.; Lach, R.; Michler, G. H. *Polym Compos* 2004, 25, 521.
8. Wu, S. *J Appl Polym Sci* 1983, 21, 699.
9. Wu, S. *Polymer* 1985, 26, 1855.
10. Ishikawa, M.; Chiba, I. *Polymer* 1990, 31, 1232.
11. Yanagase, A.; Ito, M.; Yamamoto, N.; Ishikawa, M. *J Appl Polym Sci* 1996, 60, 87.
12. Yanagase, A.; Ito, M.; Yamamoto, N.; Ishikawa, M. *J Appl Polym Sci* 1996, 62, 1387.
13. Matsuda, Y.; Hara, M.; Mano, T.; Okamoto, K.; Ishikawa, M. *Polym Eng Sci* 2005, 45, 1630.
14. Matsuda, Y.; Hara, M.; Mano, T.; Okamoto, K.; Ishikawa, M. *Polym Eng Sci* 2006, 46, 29.
15. Tang, T.; Huang, B. *J Polym Part B: Polym Phys* 1994, 32, 1991.
16. Kowalewski, T.; Ragosta, G.; Martuscelli, E.; Galeski, A. *J Appl Polym Sci* 1997, 66, 2047.
17. Kondo, T.; Sawatari, C.; Manley, R. S. J.; Gray, D. G. *Macromolecules* 1994, 27, 210.
18. Brown, E. E.; Laborie, M. P. G. *Biomacromolecules* 2007, 8, 3074.
19. Endo, T.; Kitagawa, R.; Zhang, F.; Hirotsu, T.; Hosokawa, J. *Chem Lett* 1999, 28, 1155.
20. van der Wal, A.; Gaymans, R. J. *Polymer* 1999, 40, 6045.
21. Uotila, R.; Hippel, U.; Paavola, S.; Seppälä, J. *Polymer* 2005, 46, 7923.